UCRL-PROC-226687

LAWRENCE LIVERMORE NATIONAL LABORATORY

The effect of pulse duration on laser-induced damage by 1053-nm light in potassium dihydrogen phosphate crystals

D. A. Cross, M. R. Braunstein, C. W. Carr

December 10, 2006

Boulder Damage Symposium
Boulder, CO, United States
September 27, 2006 through September 27, 2006

The effect of pulse duration on laser-induced damage by 1053-nm light in potassium dihydrogen phosphate crystals

D.A. Cross[a,b], M.R. Braunstein[b], and C.W. Carr[a,*]
[a]University of California, Lawrence Livermore National Laboratory,
7000 East Avenue, Mail Stop L-592, Livermore, CA 94550
[b]Department of physics, Central Washington University
400 E University Way Ellensburg, WA

Abstract

Laser induced damage in potassium dihydogen phosphate (KDP) has previously been shown to depend significantly on pulse duration for 351-nm Gaussian pulses. In this work we studied the properties of damage initiated by 1053-nm temporally Gaussian pulses with 10ns and 3ns FWHM durations. Our results indicate that the number of damage sites induced by 1053-nm light scales with pulse duration (τ) as $(\tau_1/\tau_2)^{0.17}$ in contrast to the previously reported results for 351-nm light as $(\tau_1/\tau_2)^{0.35}$. This indicates that damage site formation is significantly less probable at longer wavelengths for a given fluence.

Keywords: KDP, KH2PO4, crystals, laser, damage, pulse scaling,

Since the 1970's, potassium dihydrogen phosphate (KDP) have been used as frequency conversion crystals in a variety of laser systems.[1,2,3] KDP is especially suited for use in large-aperture laser systems due to the ability to grow single crystals to a large size (~700kg) with growth rates exceeding 10mm per day.[4,5] The use of KDP in a laser system can limit the maximum system fluence. The limitation arises because KDP tends to damage at fluences lower than other typical optical materials used in such systems.[6,7,8] Damage in KDP is primarily manifested as discrete localized micro-cavities in the bulk of the crystal.

As seen in figures 1 and 2, these micro-cavities, commonly referred to as pinpoints, have a complex morphology composed of subtly modified outer regions surrounding a predominant core[9,10] (see figure 2). The pinpoints depicted in figures 1 and 2 were observed on different samples and were produced under different experimental conditions; however, these pinpoints are representative of bulk pinpoints observed in KDP. While pinpoints do not continue to grow on successive shots of the same fluence level, those created on the initial shot are problematic because they scatter an amount of light proportional to the density of pinpoints and their size.[11,12] While the actual amount of energy lost due to scattered light is small, pinpoints in large numbers can create intensity fluctuations from their collective scatter (contrast) which enhances the likelihood of damaging components downstream in a laser system.[6,7,13]

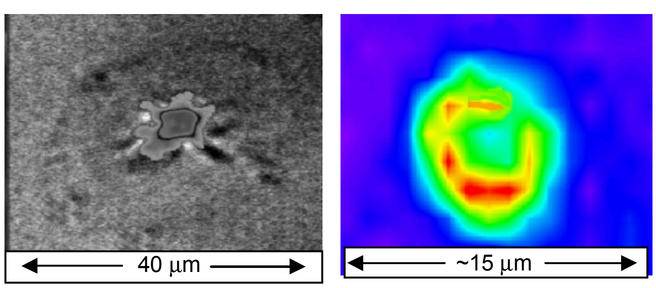

Figure 1 Left: Enhanced microscope image taken of a representative bulk pinpoint. Right: Raman scattering false color image taken after cleaving the crystal.

*Direct correspondence to C.W.Carr carr19@llnl.gov

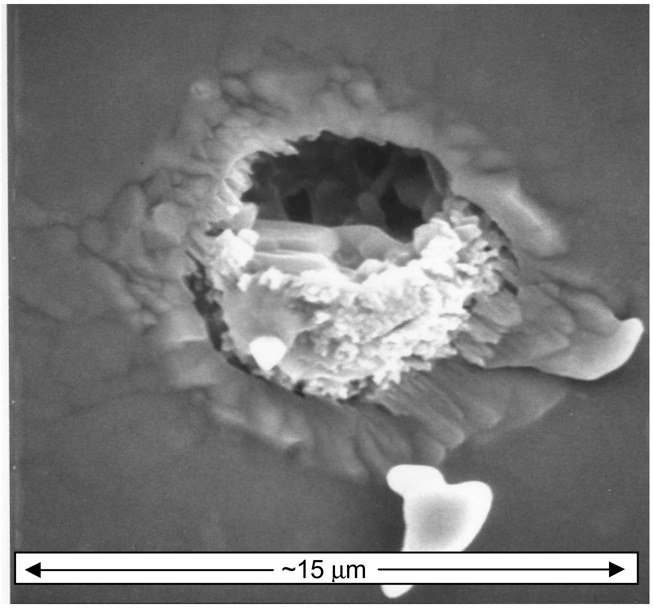

Figure 2 Scanning electron microscope image of a bulk damage site. The image was acquired after cleaving the crystal.

For pinpoints induced by 351-nm (3ω) light, size and density have been shown to depend on laser parameters such as pulse length, pulse duration, pulse shape, and fluence.[4,9,10,14,15] Both pinpoint size and density have been shown to vary with pulse duration for a fixed fluence. It has been previously demonstrated that the pinpoint density as a function of fluence, $\rho(\phi_1)$, measured for one pulse duration (τ_1) may be used to estimate the damage produced as a function of fluence by a second pulse duration (τ_2).[16,17] This estimate is commonly referred to as 'pulse scaling' and has a from of

$$\rho(\phi_2) = \rho\left(\phi_1 \times \left(\tau_1/\tau_2\right)^{\alpha}\right) \tag{1}$$

where α is the pulse scaling constant. Previously, pulse scaling for 3ω and 2ω (527nm) light has been investigated.[11,15,18] In this work we investigate the effect of pulse duration on 1053-nm (1ω) light on both pinpoint density and size.

The experimental setup is described in detail elsewhere, and is shown below in figure 3.[19] Briefly a 5cm x 5cm x 1cm Z-cut crystal sample was tested with 1053-nm temporally Gaussian pulses with FWHM durations of 3ns and 10ns. Each test was conducted on a volume of crystal not previously exposed to laser radiation.

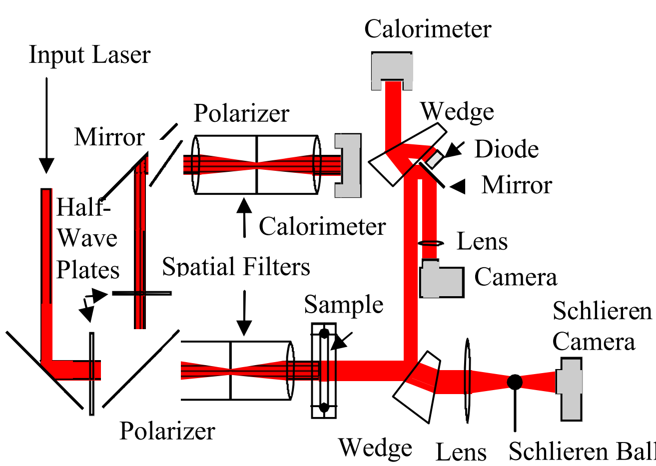

Figure 3 Experimental diagram of 1ω damaging laser system depicting energy meters and ccd cameras used to obtain nearfield fluence images and dark field scatter images.

For each shot, an image of the laser near-field was captured by a CCD camera imaged on the sample plane. This image must be calibrated for use as spatial distribution of laser fluences, as will be discussed below. The first step in calibrating the raw CCD image is subtraction of a background image. We will refer to the resulting image as the background corrected image, or for simplicity, the corrected image. The laser energy represented by a single pixel count in the corrected image is determined by dividing the pulse energy by the total counts of the image. The local fluence (at any given pixel) is then determined by multiplying the energy per count by the CCD counts of a pixel and dividing by the area of the pixel. This process repeated on each pixel of the corrected image yields a spatially resolved measure of the fluence which we will refer to as the 'fluence map'.

The damage induced in the crystal by the laser pulse is measured in two ways. A qualitative measure of the damage is recorded by taking a dark-field light scattering image of the damage. This type of image is easily obtainable by illuminating the crystal on the edge and capturing a digital image using a digital SLR with a macro-lens. If the damage observed in the digital image appears of appropriate density to a trained eye we then proceed to a more arduous, but far more quantitative measurement using a robotic microscope. The microscope uses integrated blob recognition software in conjunction with 3-axis movement to record the size and location of all pinpoints in a prescribed volume. The detection limit of the technique for densities less than ~ 50 pinpoints / mm^3 of the technique is ~ 1 μm diameter pinpoints. At higher damage densities the ability to detect small pinpoints is greatly reduced.

An x/y bubble plot, in which each pinpoint is plotted at its x/y location with a dot proportional to its diameter, provides a visualization tool for the collected data. It is important to note that because theses experiments are conducted with a single wavelength (and not during frequency conversion), the fluence does not vary appreciably with depth in the crystal. An implicit assumption in the data analysis is that the depth information of the damage sites can be discarded. In figure 4 the fluence map, dark field image of the damage, and a bubble plot of the damage can be compared.

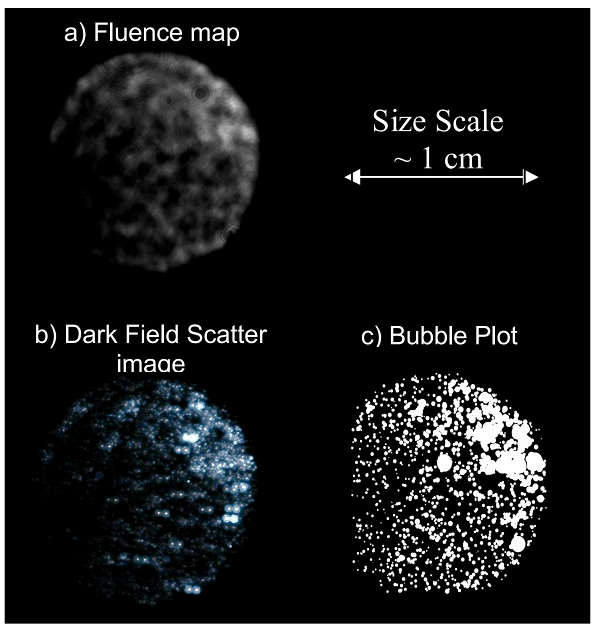

Figure 4 a) Fluence map of a 3-ns shot b) Dark field scatter image taken with side illumination c) The size and location of the pinpoints in the damage volume are plotted in two dimensions as circles proportional to pinpoint diameter.

As seen in figure 4, both the fluence of the pulse as well as the corresponding damage in the crystal varies laterally over the sub-aperture. Because the local values of both fluence, and average pinpoint density are known, we are able determine pinpoint density as a function of fluence from a single test site. The fluence image is registered to the damage density by assuming higher fluences will produce a higher density of damage and utilizing the patterns in the beam fluence map and corresponding features in the damage density. A simple code was written to calculate and collate the pinpoint density and average fluence from the fluence map and the list of pinpoint locations collected with the automated microscope. Local density was determined by counting the number of pinpoints in 417-μm x 417-μm regions (at all depths) and dividing by the volume of 1.74 mm^3 (crystal thickness was 10 mm). A bin size of 417-μm was chosen because this length corresponds to 10 x 10 pixels in the fluence near-field image and is below the correlation length for fluence fluctuations of more than ~10%. The resulting pinpoint density plotted as a function of fluence $\rho(\phi)$ and fit to allometric relationship is shown in figure 5.

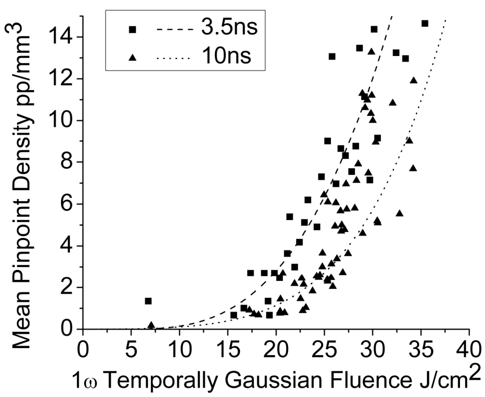

Figure 5 Local damage density plotted vs. local fluence for 1ω temporally Gaussian pulses of 3ns and 10ns duration.

To describe the effect of pulse duration on damage density the pulse scaling constant α from equation 1 must be determined. This constant was obtained by performing a least squares fit between the 3.5ns and 10ns pulse duration data sets. As stated above the $\rho(\phi)$ data for each pulse duration is fit to allometric functions. This function is of the form:

$$\rho(\phi) = A\phi^b \tag{2}$$

where A and b are constants. A least squares fit between the pulse durations is accomplished by first fitting the 3.5 ns data to the form of equation 2. Next, the 10ns data is also fit to an allometric relationship making use of the constants obtained from equation 2 and the scaling factor from equation 1. Thus the 10ns data is fit to a function of the form:

$$\rho(\phi) = A(\phi\kappa)^b \qquad where \qquad \kappa = \left(\tau_1 / \tau_2\right)^\alpha \tag{3}$$

with the constants A and b equal to the constants obtained from equation 2; τ_1 and τ_2 are the pulse durations 3.5ns and 10ns respectively. This least squares fit provides a pulse scaling constant for 1ω light to be α=0.17±0.05. This contrasts with previously reported results for 2ω and 3ω pulses of durations between 1-ns and 10-ns for which fluence scaled with α~0.3 for 2ω and α~0.35 for 3ω, and indicates that the amount of damage initiated with 1ω light is much less sensitive to pulse duration.[15,18]

Previous measurements of the damage threshold as a function of wavelength revealed discrete steps in the damage threshold at fractions of the band gap. Theses steps were attributed to the absorption properties of the material being dominated by defect assisted multi-step absorption.[20] In brief this model suggests that electrons are elevated from the valance band in a series of transitions to the conduction band or defect states just below the conduction band. The difference in the number of steps needed to elevate the electrons as a function of wavelength would also require different values of α for wavelengths with different absorption order, such as for 1ω, 2ω, and 3ω light.

Acknowledgements

The authors would like to thank Richard Hackel of LLNL for his repeated proofreading of the manuscript. Work performed under the auspices of the U.S. Department of Energy by the University of California, Lawrence Livermore National Laboratory under contract No. W-7405-Eng-48.

References

[1] K. Kato, Optics Communications **13** (2), 93 (1975).
[2] R. S. Craxton, S. D. Jacobs, J. E. Rizzo et al., IEEE Journal of Quantum Electronics **17** (9), 1782 (1981).
[3] M.M Fejer Physics Today **47** (5), 25 (1994).
[4] B. C. Stuart *et al.*, Phys. Rev. B, Condens. Matter (USA) **53**, 1749 (1996).

[5] N. P. Zaitseva, J. J. DeYoreo, M. R. Dehaven et al., Journal of Crystal Growth **180** (2), 255 (1997).
[6] C.W. Carr, M. Johnson, M. D. Feit, and A. M. Rubenchick, Applied Physics letters (In Press).
[7] C.W. Carr, M. D. Feit, and A.M. Rubenchick, presented at the Boulder Damage 2004 (unpublished).
[8] N. Bloembergen, IEEE Journal of Quantum Electronics **QE-10** (3), 375 (1974).
[9] H. Yoshida *et al.*, Appl Phys B-Lasers Opt **70**, 195 (2000).
[10] A. K. Burnham *et al.*, Appl. Opt. (USA) **42**, 5483 (2003).
[11] C.W. Carr, M. Staggs, H. B. Radousky et al., 2003 (unpublished).
[12] S. G. Demos, M. Staggs, M. Yan et al., 1999 (unpublished).
[13] M. D. Fiet, et al., SPIE 4347,383 (2001)
[14] M. Runkel *et al.*, in Boulder Damage Symposyem (SPIE, Boulder, CO, 2001), p. 359.
[15] Adams J.J., Weiland T.L., Stanley J.R., Sell W.D., Luthi R.L., Vickers J.L., Carr C.W., Pulse length dependence of laser conditioning and bulk damage in KD_2PO_4 SPIE **5647**, 265 (2004)
[16] A. K. Burnham, M. Runkel, M. D. Feit et al., Applied Optics **42** (27), 5483 (2003).
[17] E. W. Vanstryland, M. J. Soileau, A. L. Smirl et al., Physical Review B **23** (5), 2144 (1981).
[18] M.D. Feit, A.M. Rubenchik, A. Salleo et al., Laser-Induced Damage in Optical Materials: 1997, Proceedingsof SPIE **3244** (1998).
[19] P. DeMange, C.W. Carr, H.B. Radousky, S.G. Demos, Review of Scientific Instruments **75**, 10 (2004)
[20] C. W. Carr, H. B. Radousky and S. G. Demos (2003). Physical Review Letters **91**(12): 127402.